IOP PUBLISHING EUROPEAN JOURNAL OF PHYSICS

Eur. J. Phys. **28** (2007) S13–S27 doi:10.1088/0143-0807/28/3/S02

Using Peltier cells to study solid–liquid–vapour transitions and supercooling

Giacomo Torzo[1], Isabella Soletta[2] and Mario Branca[3]

[1] ICIS-CNR and Physics Department of Padova University, Padova, Italy
[2] Liceo Scientifico Fermi, Alghero, Italy
[3] Chemical Department of Sassari University, Sassari, Italy

E-mail: torzo@padova.infm.it, isasolet@tin.it and branca@uniss.it

Received 28 September 2006, in final form 8 November 2006
Published 30 April 2007
Online at stacks.iop.org/EJP/28/S13

Abstract

We propose an apparatus for teaching experimental thermodynamics in undergraduate introductory courses, using thermoelectric modules and a real-time data acquisition system. The device may be made at low cost, still providing an easy approach to the investigation of liquid–solid and liquid–vapour phase transitions and of metastable states (supercooling). The thermoelectric module (a technological evolution of the thermocouple) is by itself an interesting subject that offers a clear example of both thermo-electric (Seebeck effect) and electro-thermal (Peltier effect) energy transformation. We report here some cooling/heating measurements for several liquids and mixtures, including water, salt/water, ethanol/water and sodium acetate, showing how to evaluate the phenomena of freezing point depression and elevation, and how to evaluate the water latent heat.

(Some figures in this article are in colour only in the electronic version)

1. Introduction

Introductory courses in thermodynamics are normally focused on the study of equilibrium states that may be described through a reduced number of macroscopic variables and form the necessary base for a general understanding. Similarly the quasi-static transformations, defined by infinitesimal heat exchanges with ideal reservoirs with infinite thermal capacity, are usually studied.

In contrast, in real laboratory experiments, quasi-static transformations or ideal heat reservoirs do not exist and frequently we do not reach true equilibrium states.

In the present paper we describe an apparatus that, exploiting Peltier cells and a real-time data acquisition system, makes possible to study several transformations that proceed through non-equilibrium states, allowing a rather deep insight on the investigated processes.

One advantage of the set-up described here is that the time required to carry out one experiment is normally in the range from 10 to 20 min, well within the 45 min typically available for lab class experiments.

2. Metastable states. Supercooling

The common idea of equilibrium is based on the experience that any system tends to evolve to a state of minimum energy in which its macroscopic behaviour becomes stable. Therefore a system that exhibits a stable behaviour is normally assumed to be an equilibrium state.

However, we know that some long-lived states that appear to be equilibrium states are instead metastable states that may evolve into states of lower free energy. This may occur spontaneously, or may be necessarily an external triggering phenomenon. Examples of metastable states requiring an external trigger are chemical mixtures (such as gunpowder or mixtures of explosive gases, which react after sufficient heat input), or more simply any *supercooled* liquid.

Supercooling in water is a phenomenon known for a long time [1]; it was first observed by Daniel Gabriel Fahrenheit in 1724, and later by Joseph Black. But almost any liquid can be cooled to a metastable state by a sufficiently rapid cooling through the freezing point [2]. The solid phase grows from the liquid phase by increasing the size of initial crystalline clusters. These crystal seeds on the other hand may form only by passing over an energy barrier due to the large surface-to-volume ratio of any small object. In the absence of such crystal seeds the liquid phase may be maintained at temperatures much lower than the freezing point. Supercooled water may exist down to $-40\ ^{\circ}$C. However, ice may form at higher temperature, depending on the cooling speed and on the presence of impurities that favour crystal seeds formation.

A popular supercooled liquid at room temperature [3] is the tri-hydrated sodium acetate ($NaCOOCH_3\ 3H_2O$), whose large latent heat produces huge temperature changes that are easily observed even without any measuring device, for example in the '*hand-warmer bags*'.

3. Experimental set-up

The experimental set-up was designed to obtain, at low cost[4] a useful temperature range from $-20\ ^{\circ}$C to $120\ ^{\circ}$C with a liquid sample volume of about 10 cm^3. This allows us to investigate both freezing transitions and boiling temperatures in several common liquids, with easy measurements that can be normally completed within half an hour.

The working principle of thermoelectric devices (Peltier cells) was well described in this Journal by Kraftmakher [4] and it will not repeated here.

The system (see figure 1) is made of a sample holder (an aluminium pot) which is thermally coupled to the 'cold plate' of a Peltier stack (made of two cells connected in series); the 'hot plate' of the stack is thermally coupled to an aluminium heat sink, linked to room temperature by a standard PC blower.

A real-time data-acquisition system monitors the temperatures of sample, cold and hot plates during cooling/heating runs, allowing us to graph, not only the time evolution of the sample, but also the temperature gradients in different parts of the device.

[4] The total cost of the components, excluding the power supply and the data acquisition system, is less than 100 euro.

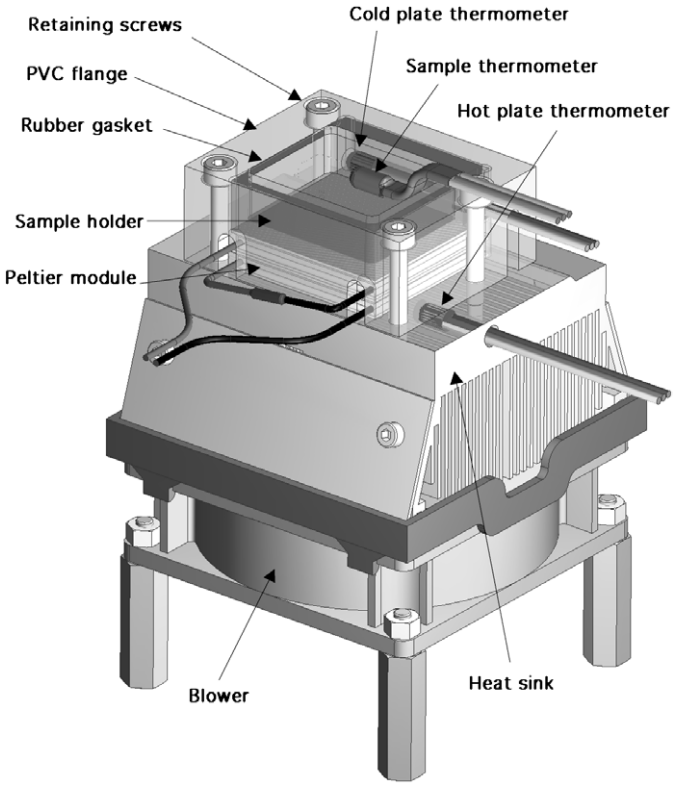

Figure 1. Schematic picture of the experimental set-up. (Not shown the neoprene insulating cap, the power supply and the data acquisition system).

3.1. The thermoelectric module

We use two identical cells instead of a pyramidal stack to simplify the device construction and thermal insulation. The multi-stage cooling modules are in fact usually configured with a smaller cell on the cold side and a larger one at the hot side because the larger cell must pump also the energy dissipated by the Joule effect that adds to the energy transferred by the smaller cell. We selected the cheap model [5] Pke128a0020 (http://www.opitec.it) whose dimensions are $40 \times 40 \times 4.7$ mm, with a nominal maximum power of 33 W.

The heat sink is a commercial component, commonly used to cool the computers CPU, which is sold with forced ventilation provided by a 12 V dc blower.

The sample holder is a square aluminium pot, dimensioned to match the geometry of the Peltier cells minimizing the surface area of the sample holder subject to moisture condensation and to radiation/convection thermal coupling with the ambient. It has 9 mm inner height, 3 thin walls (2 mm) and a thicker one (8 mm), where a hole is drilled to host a thermometer. A second thermometer is suspended inside the pot to monitor the sample temperature, and a third thermometer is placed in a hole drilled on the aluminium heat sink.

If the thermal coupling between the sample holder and the 'cold plate' and between the heat sink and the 'hot plate' is good enough, we may assume the first thermometer measures the temperature of the cold plate and the third thermometer measures the temperature of the hot plate.

The role of 'cold' and 'hot' plates obviously is exchanged when passing from cooling run to heating run.

The Peltier cells are thermally anchored to the sample holder and to the heat sink by using thermally conductive grease and by *applying a strong pressure* to the contacting surfaces.

An important part of the device is the PVC flange, with a rectangular top aperture and four retaining screws, that presses the 'sandwich' made of the sample holder plus the two Peltier cells, against the heat sink.

An elastic sealing, obtained from a rubber sheet 2 mm thick, maintains the high pressure, applied at room temperature, despite the changes of the geometry induced by different thermal expansion coefficients in cooling/heating processes.

An outer (removable) cap made of insulating material (neoprene foam) covers the sample holder to reduce the thermal coupling with the ambient during the measurements.

3.2. The data-acquisition system

We adopted the LabPro interface from Vernier (http://www.vernier.com), connected to a PC through USB port, that offers a very good cost/performance ratio, but similar products are perfectly suited for our set-up, for example those produced by PASCO Scientific (http://www.pasco.com) or CMA (http://www.cma.science.uva.nl).

One advantage of the adopted interface is that it may also be used replacing the personal computer with a handheld graphic calculator, e.g. the Texas Instrument TI92, or TI89, or TI-Voyager (see the examples shown in the LEPLA Minerva Project at http://www.lepla.eu).

3.3. The thermometers

We used as temperature sensors the integrated-circuits National LM61 in a plastic TO92 envelope (4.5 mm diameter, 5 mm length), with a *nominally* constant sensitivity of +10 mV K^{-1} and an output offset of +600 mV at $T = 273$ K.

The transfer function (calibrating equation) for this sensor is therefore $T\,(^{\circ}\mathrm{C}) = \mathrm{V}{*}100{-}60$.

The offset allows reading negative temperatures without the need for a negative supply: the three-wire sensor in fact may be powered by the 5 V output supplied at the interface analogue input (raw-voltage mode, range 0–5 V). No special skill is required for interfacing this analogue sensor: only a cable with BT plug on one end must be used, and proper connections of the three sensor pins (ground, +5 V, output), as specified in the LabPro manual. It must also be noted that the wires connecting the sensor to the BT cable must be thin (e.g. 30AWG), in order to reduce the thermal link between the sensor and room temperature.

One detail is very important, that is, the sample thermometer must be carefully placed horizontally *at the free surface* of the liquid; therefore its position must be re-adjusted when the sample volume is changed. In fact, if the sensor is completely immersed in the liquid sample, it does not faithfully measure the temperature of the liquid–solid mixture when the solid–liquid interface (that moves in the bottom–top direction) reaches the thermometer height. On the other hand if the sensor only touches the liquid surface the thermal coupling with the sample becomes poor.

We fixed the sensor, by a heat-shrinkable tube, to one end of a metal wire. The other end of the wire is loop-shaped and blocked by one of the four retaining screws; by properly bending the wire, the sensor may be positioned at the required height.

The poor nominal accuracy of LM61B (a *maximum* error of 3 °C and a *typical* error of 1 °C in the range −30 °C +100 °C) is mostly due to deviations from linearity, and this does not prevent reliable evaluation of temperature *differences* smaller than 1 °C. We tested several

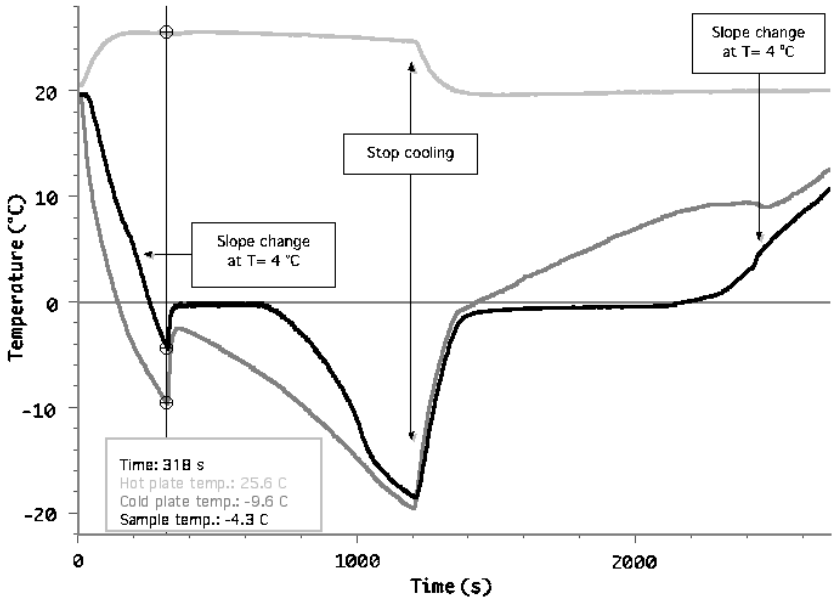

Figure 2. The temperature of the 12 cm^3 water sample as a function of time. Black line: temperature T_1 (sample); dark grey line: temperature T_2 (sample holder); light grey line: temperature T_3 (heat sink).

units and we found that the spread in the values of the measured temperatures was always less that 0.6 °C in the full range.

3.4. Power supply

The current supplied to the Peltier cells to transfer heat from the cold plate to the hot plate, (or vice versa, depending on the sign of the Peltier bias voltage) is fed by a power supply (e.g. 0–30 V, 0–3 A).

The only requirement for the power supply is a *small output ripple*, and it may operate either at constant voltage or at constant current. A commercial (wall-plug) power supply with 12 V dc output feeds the blower.

4. Exploring phase transitions in various systems

The introductory experiment should be carried out using a sample of water. This makes easier the students' understanding of the results, and moreover the collected data may be later used for a calibration of the effective heat capacity of the system (see section 5). Later the students may explore more complex systems, such as binary mixtures.

4.1. Supercooling of water

In figure 2 we report the result obtained while cooling a 12 cm^3 water sample. The black curve marks the temperature T_1 of the sample, as measured by a sensor placed horizontally inside the water, but close to the free surface. The dark-grey curve traces the temperature T_2 of the

aluminium pot, which is in good thermal contact with the cold plate of the Peltier cell. The light-grey curve traces the temperature T_3 of the hot plate.

The shown cooling run starts from room temperature (20 °C) with the power supply feeding 1.4 A current, at 11 V, to the Peltier module. By recording also the temperature of the cold plate we may evaluate the temperature difference $\Delta T = T_1 – T_2$ across the sample volume.

The temperatures measured by the sample and cold plate thermometers decrease following a nearly exponential curve due to the increasing thermal leak that steadily lowers the net heat transfer from the cold plate to the hot plate.

Near $T_1 = 4$ °C we may observe a slight change in the slope, and a reduction of ΔT (that will decreases to about 5 °C at $t = 300$ s). This phenomenon is due to the anomaly of the water density at $T = 4$ °C [6].

When cooling the sample from the bottom, at the beginning the lower water layers (cooler) are denser than the higher layers, and no convective flow contributes to the heat exchange within the fluid sample. The small thermal conductivity of water (0.56 W m^{-1} K^{-1} to be compared with the values 0.7 W m^{-1} K^{-1} for glass and 2.3 W m^{-1} K^{-1} for ice [7]) maintains a large gradient $\Delta T \approx 8$ °C. As soon as the water maximum density is crossed at about $T = 4$ °C, the water bottom layers (cooler) become lighter than the layers above (warmer), an convective flows begins, reducing the temperature gradient within the sample volume.

At $t \approx 250$ s, the water temperature crosses the 0 °C value without freezing: supercooling begins. The sample enters into a metastable state, remaining liquid at temperatures below the freezing temperature. In the run reported in figure 2 the metastable state collapses at $t = 318$ s, showing a steep rising, followed by a plateau at $T = 0$ °C.

Also the cold plate temperature T_2 increases rapidly, proving that the water has transferred a large amount of heat to the container. This energy is released by the sudden freezing the water layers close to the aluminium walls. The heat flush is so large that even the hot plate marks a slight temperature rise at the time $t = 318$ s, as shown by the light-grey curve T_3.

On the plateau region, the top liquid water layers behave as a powerful heat source (*latent heat*) for the underlying solid water layers. All the energy drained by the bottom layers is supplied by the phase change so that the liquid temperature remains constant, while the cold plate temperature keeps on cooling at a smaller rate.

From $t = 340$ s to $t = 690$ s, the T_1 curve is flat, then it starts bending, even if part of the sample is still liquid. This is due to the fact that the thermometer is partially coupled to the solid phase, which is not isothermal (a strong gradient affects the ice layers due to the large heat transfer).

Finally, near the time $t = 750$ s, almost all the liquid has been frozen, and ΔT is about 7 °C. The completion of freezing is marked by a slight increment in the slope of the cold plate temperature curve; at this time the heat load at the cold plate side (missing the latent heat of solidification) is due only to the specific heat of ice. This last feature is more visible when the power supply to the Peltier cells is increased (see, for example, the similar plot in figure 10).

When the phase transition is completed in the whole volume, the T_1 and T_2 curves get closer until (at $t > 1100$ s) the temperature difference becomes quite small ($\Delta T < 1$ °C), due to the fact that the thermal conductivity in ice is five times larger than in water. The residual small gradient is due to the heat leaking to the sample thermometer from the top (radiation, air convection and conduction through the thermometers wires).

At $t = 1200$ s the power supply of the Peltier cell is switched off and the heat flow is inverted because the inactive thermoelectric device is a good thermal conductor that links the sample holder to room temperature. Because now the major part of heat is supplied to the cell from bottom, the anomaly at $T = 4$ °C now inhibits the convection below 4 °C and induce convection above 4 °C. The effect of the increased thermal coupling due to convective flow is

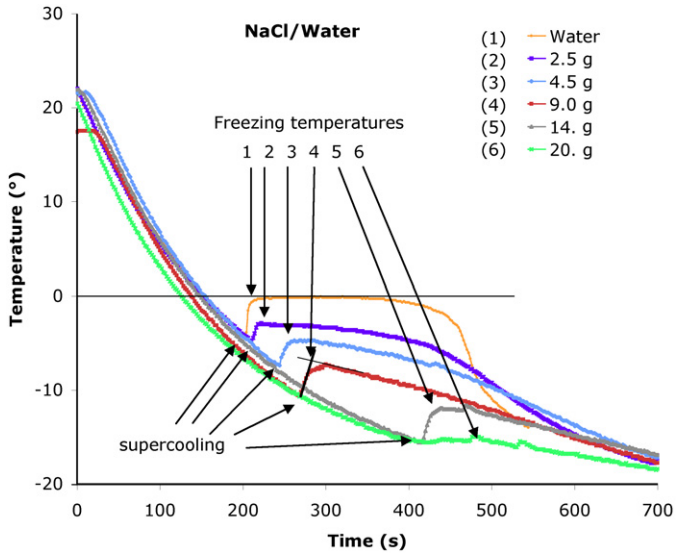

Figure 3. Temperature of salt/water mixtures as a function of time. The legend shows the quantities of NaCl dissolved per 100 g of water in different samples.

also marked by a change in the slope of T_2. As a result the temperature difference drops from $\Delta T = -8\ ^\circ\mathrm{C}$ at $t = 2300$ s to $\Delta T = -4\ ^\circ\mathrm{C}$ at $t = 2500$ s.

This short series of data includes a large amount of information and hints for classroom discussions. It may introduce the students to a critical reading of plots and to a refining of analysis. The data also reveal unexpected details, not shown in textbooks that normally discuss ideal situations where transformations are quasi-static and involve homogeneous samples.

4.2. Water/salt mixtures

The water/salt mixture is a system particularly suited for educational experiments [8]; it is a common system with important applications in physics, chemistry and biology. It is part of the common knowledge both of teachers and of students. The $NaCl/H_2O$ mixtures are easy to be prepared, using tap water and kitchen salt, without any special prerequisite or sophisticated laboratory tools, and therefore they may be proposed for experiments both for introductory courses in university science labs, or even in secondary high schools.

In the following we describe some results, obtained using our apparatus to show firstly the *freezing point depression* in solutions (as well as the supercooling effect), then the *boiling point elevation*.

In figure 3 we report several cooling runs taken with mixture with increasing salt content. By increasing the NaCl concentration the freezing temperature decreases, showing clearly the phenomenon of freezing point depression. From these data the students may infer how much salt must be used to melt out the ice on the streets in the case of very cold winter!

We observe that while in pure water the freezing plateau maintains a rather constant temperature, in salt solutions the temperature clearly decreases with time. This effect is due to the change in concentration during freezing. Therefore the freezing temperatures must be extrapolated [9] from the cooling curves, as shown in figure 3 (curve 4).

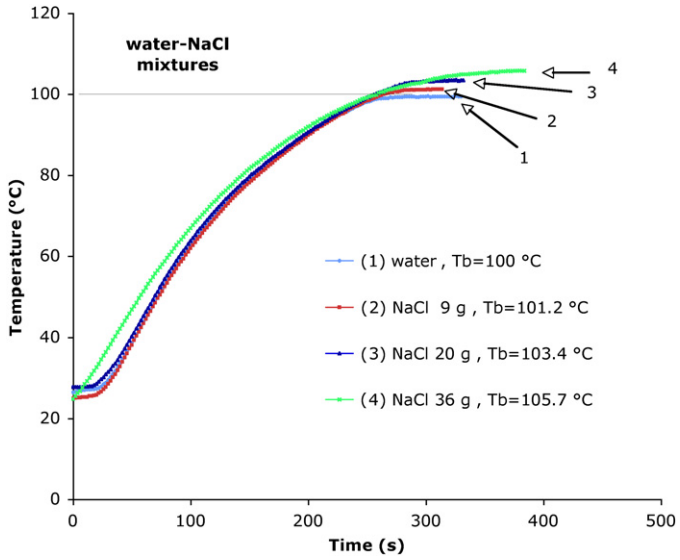

Figure 4. Temperature of salt/water mixtures as a function of time. The legend show the quantities of NaCl dissolved per 100 g of water in different samples.

Table 1. (∗) Values derived from the eutectic plot of the NaCl/water mixture.

Weight (g)	Weight (%)	T peak value (°C)	T extrapolated value (°C)	Reference [11] (∗) (°C)
0	0	0,2	0,2	0
2.5	2	−3	−2	−1
4.5	4	−5	−3	−2
9.0	8	−7	−6	−5
14.0	12	−12	−10	−9
20.0	17	−15	−13	−13

Despite the relative simple procedure here used, the results are in fair agreement with data reported in the literature [10], as shown in table 1.

In the sample with maximum concentration (here 20 g of salt in 100 g of water corresponds to a NaCl concentration of 17%, slightly lower than the eutectic concentration of 23%) the supercooling effect almost disappears, probably because at the lowest temperatures the cooling speed becomes low enough to allow crystal seeds nucleation at a temperature close to the freezing point.

Using the same apparatus, by simply reversing the sign of the current supplied to the Peltier cells, we may explore also the phenomenon of the *boiling point elevation*.

In figure 4 we report several heating runs taken with mixture with increasing salt content.

By increasing the NaCl concentration the boiling temperature increases from 100 °C up to about 106 °C at the saturated solution (36 g of salt in 100 g of water corresponds to the maximum NaCl concentration of 26.5%).

Here we may compare the measured values of the boiling temperature in different samples $T(m) = T_b + \Delta T$ with those predicted by the formula $\Delta T = i\, K_b \cdot m$, where T_b is the boiling point for the solvent, K_b is the boiling point elevation constant and m the molal concentration

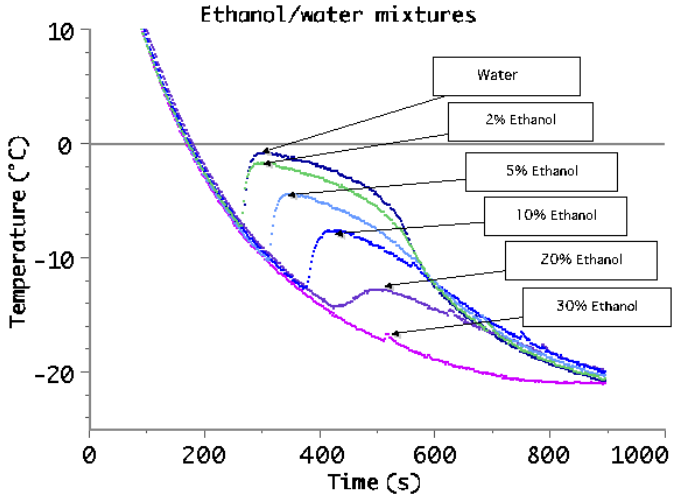

Figure 5. Temperature of ethanol /water solutions as a function of time. The legends show the fractions of ethanol content in different samples.

Table 2.

Weight (g)	$i \cdot m$	Measured ΔT (°C)	$\Delta T = \mathrm{K_b} * \mathrm{m}$ (°C)	ΔT (Reference [13]) (°C)
9	3.08	1.2	1.6	1.5
20	6.84	3.4	3.6	3.5
36	12.32	5.7	6.4	7.5

(i.e. the number of mole soluted per Kg of solvent), i the van't Hoff factor ($i = 2$ for the two ions in the case of NaCl).

For water [11] $K_b = 0.52$ K/(mole Kg^{-1}), and the values reported in figure 4 are compared with the calculated values and with the values accepted in the literature [12] in table 2.

This demonstrates that it is not very important which component (salt or pasta) is introduced first into the water kettle, when cooking spaghetti : the cooking temperature does not change so much . . .

4.3. Water/ethanol mixtures

The experiments described in the previous section may be used to explore other heterogeneous systems: for example, we may use water/alcohol solutions to illustrate the working principle of *fractional distillation*. We prepared the mixtures using commercial ethanol (which is a 96% alcohol/water mixture) and tap water.

Figure 5 is similar to figure 3, demonstrating both supercooling and freezing point depression.

Figure 6 is similar to figure 4, but here we may appreciate also the difference in the behaviour of pure fluids (100% water or 100% ethanol) from that of binary mixtures.

Pure fluids show a definite value for boiling temperature, because their composition is stable during the boiling process.

On the other hand, in binary mixtures the temperature at which the vapour pressure equals the ambient pressure (condition for boiling) changes with the mixture composition, which in

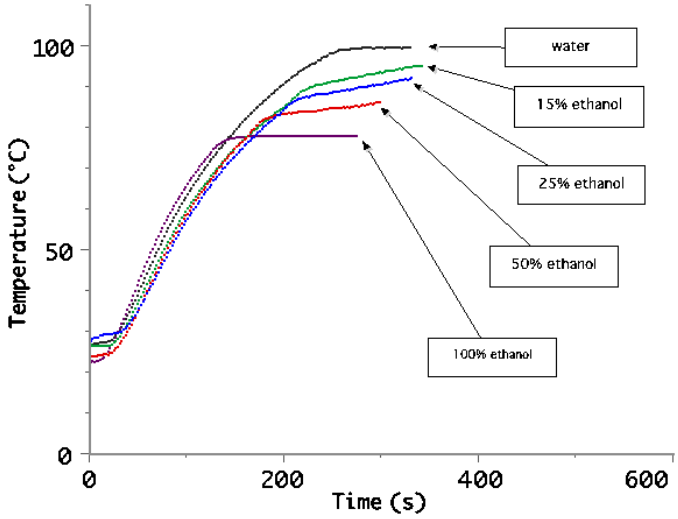

Figure 6. Temperature of ethanol/water solutions as a function of time. The legend shows the *nominal volume fraction* of ethanol content in different water samples at the start of heating.

Table 3. The effective ethanol volume fraction is calculated from nominal values assuming a starting mixture of 96% ethanol in water (commercial alcohol). The expected T_b values are taken from [14].

Ethanol volume fraction (%)	Ethanol molal fraction (%)	Expected T_b (°C)	Measured T_b (°C)
0	0	100	99.3
14.4	5.0	91	89
24	9.1	88	87
48	23.2	83	83
96	88.4	79	78

turns changes during the boiling process, because mainly the component with lower boiling temperature does evaporate.

As a consequence, the heating curves of pure fluids show a *horizontal plateau* at the boiling temperature, while mixture's heating curves show only a *change in slope* when boiling begins.

Table 3 compares the measured values of the measured boiling temperatures (the temperatures where the T_1 curves change slope) and the expected values [13].

4.4. Supercooling of sodium acetate

A cooling run with sodium acetate does not offer substantial news about supercooling, but it may amaze the students with the very large amount of heat that the sample delivers when the metastable liquid relaxes into the solid phase.

Figure 7 shows an example of such transition where the sample temperature jumps up about 70 °C in few seconds (from −15 °C to 54°C). The temperature rise would be even larger if the sample would not be thermally coupled to the aluminium holder: part of the heat flush is in fact transmitted to the sample holder whose temperature rise is about 13 °C.

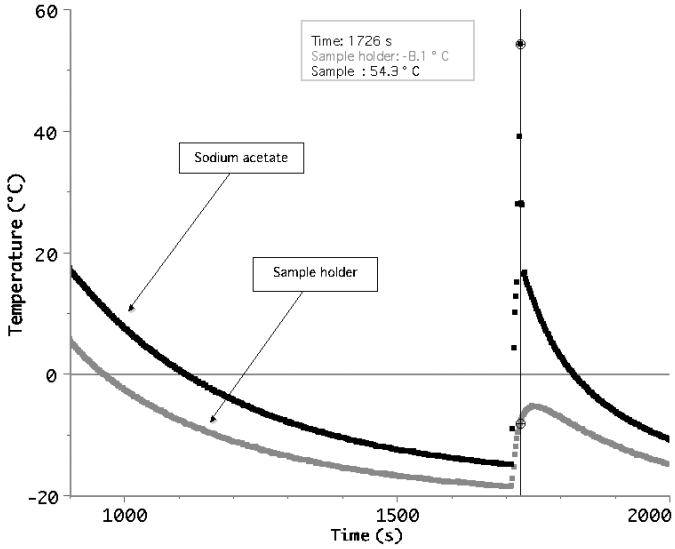

Figure 7. Supercooling of sodium acetate Black line: sample temperature; grey line: sample holder temperature.

The advantage of this fluid is that the freezing temperature (54 °C) is well above room temperature, so that we may play with the metastable liquid at room temperature (e.g. after heating it above 70 °C, and waiting for natural cooling down to room temperature). We may artificially trigger its phase change by simply adding a small crystal of sodium acetate (or by acoustically induced seed generation, as in the commercial 'thermal pads').

This system therefore does not need a Peltier device to observe supercooling, only a common heater is required for melting. However, using our apparatus it become easy and comfortable to record in a short time several cycles of cooling/heating curves where both the freezing temperature and the 'heat flush' can be observed.

In figure 8 we may see the slope change (both in the sample and in the sample holder curves) at the time when the solid sample reaches the melting temperature (54 °C). The heat subtracted to the aluminium holder (due to the latent heat of fusion) is able to temporarily cool the sample holder. The corresponding increasing of the slope in the sample temperature curve is due to the sudden increase of the thermal coupling between the thermometer and the sample. At melting, the liquid phase introduces the mechanism of convection, which drastically reduces the gradient within the sample volume.

5. Evaluation of latent heat

Using the collected data the latent heat of fusion, i.e. the thermal energy released per unit mass during the liquid–solid phase transition.

In the usual laboratory this is done by measuring the temperature drop of a known quantity of heated water when it is mixed to a know quantity of ice at 0 °C. These measurements are normally quite inaccurate [1, 14]. Some authors propose very precise and sophisticated methods, which allow measuring the latent heat even in binary mixtures, but they use an apparatus, the differential scanning calorimeter, that is not available in common teaching labs [10].

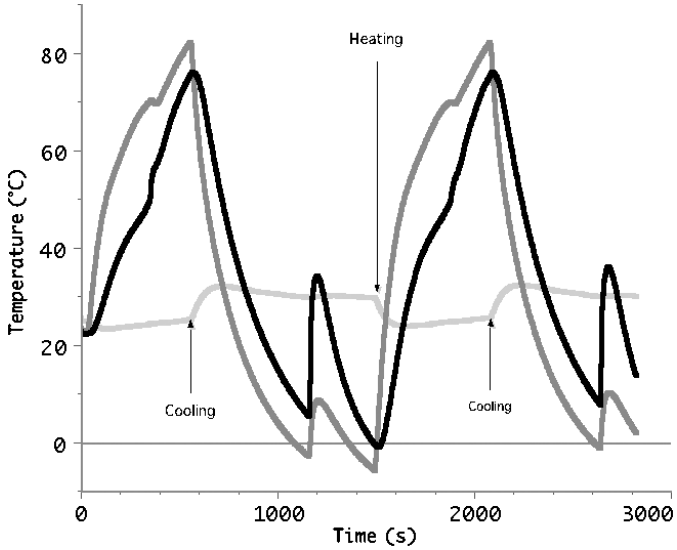

Figure 8. Repeated heating/cooling cycles of sodium acetate. Black line: sample temperature; dark-grey line: sample holder temperature; light-grey line: temperature of the Peltier cell plate coupled to room temperature by air blower.

Our method is less direct than those found in the literature but it offers a fast and easy data acquisition.

In order to evaluate the latent heat from the data taken during a liquid solid phase transition, we must know the sample specific heat c, its mass m and the effective heat capacity of the sample holder C_x.

From the slope $S = \mathrm{d}T/\mathrm{d}t$ of the cooling curve for the sample holder, measured near the freezing temperature, we evaluate the cooling power $W = S\,(c\,m + C_x)$.

The energy supplied to the sample holder in a time interval Δt, near the freezing temperature, is therefore approximated by the product $W\,\Delta t$.

Then we measure, on the sample cooling curve, the time Δt_x passed from the instant of crossing the freezing temperature until the end of the plateau (when the curve slope start increasing).

The total energy supplied to the sample is therefore $E = W\,\Delta t_x - C_x\,(T_2 - T_1)$, where T_2 and T_1 are the temperatures of the sample holder at the beginning and end of the time interval Δt_x. In our measurements this temperature difference is almost negligible, so that we may approximate the above relation with $E = W\,\Delta t_x$.

The latent heat L may be therefore calculated as

$$L = E/m = W\,\Delta t_x/m = S\,\Delta t_x\,(cm + C_x)/m.$$

The parameter C_x is greater that the nominal heat capacity $C = m_{\mathrm{al}}\,c_{\mathrm{al}}$ (calculated from its mass m_{al} and the aluminium specific heat c_{al}). The Peltier cell in fact does cool also the material that is in thermal contact with the sample holder (the cell itself, the retaining cap and the insulating cap . . .).

We may however evaluate C_x by comparing the cooling slopes of two curves, one taken with the mass m_1 of water (S_1) and the other with the empty sample holder (S_0), using the same power input for the Peltier cells. In fact from the two relations $W = S_1\,(c\,m_1 + C_x)$, and $W = S_0\,C_x$ we get

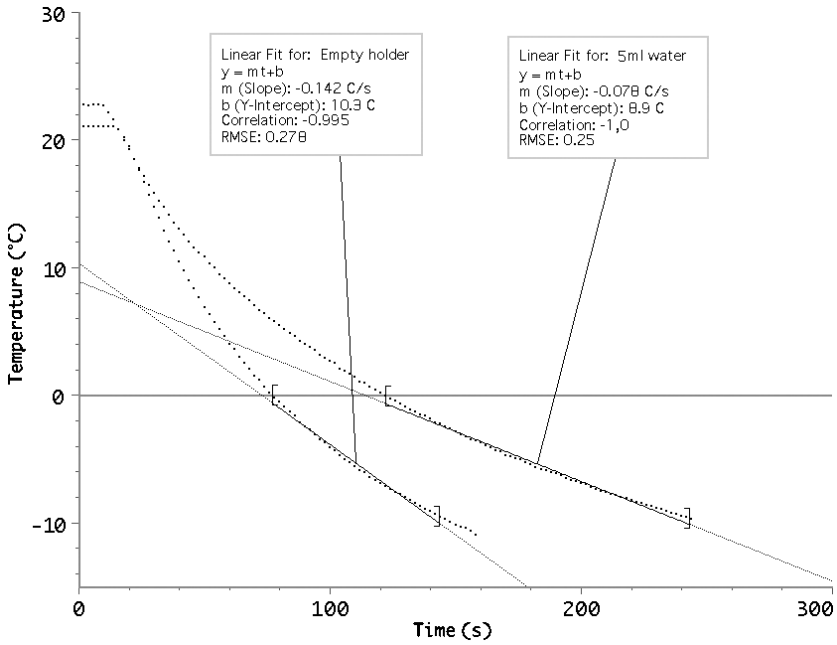

Figure 9. Procedure to calculate the effective heat capacity as explained in the text. Run taken driving the Peltier cell with $I = 1.6$ A. The data points linearly interpolated are those enclosed in the square brackets.

$$C_x = c\, m_1\, S_1/(S_0 - S_1).$$

In our apparatus the value of C_x, calculated from the two cooling runs shown in figure 9 (one with empty sample holder and one with 5 cm^3 of water) may be assumed to be about (45 ± 4) J K^{-1}, much larger than the value 18 J K^{-1} calculated for the 20 g aluminium sample holder.

Using the calculated value of C_x, the known value of the water specific heat $c = 4.18$ J g^{-1} C^{-1} and the values obtained from the cooling run reported in figure 10 [$m = (6 \pm 0.2)$ g, $\Delta t_x = (342 \pm 4)$ s, S $= 0.083 \pm 0.001$) °C s^{-1}], we obtain for the water latent heat $L = (332 \pm 38)$ J g^{-1}, a value in good agreement with the known value $L = 335$ J g^{-1}.

Note that the calculated value of C_x is a constant (it should not depend on the power applied to the Peltier cells, i.e. on the value of the heat flux drained from the sample holder).

6. Comparing Peltier and Seebeck effects

The system we have described may also be used to give practical examples of the efficiency of two energy conversion processes: the Peltier effect converts electric power into heat transfer between two reservoirs, the Seebeck effect converts the heat flux into electric power [15, 16].

This may be obtained by adding a simple option: a toggle switch, at the end of a cooling or heating run, disconnects the wires feeding the Peltier cell from the power supply and connects them to a motor driving a small propeller.

The students will see the Peltier module converted into a thermoelectric generator that exploits the thermal gradient to produce a dc current: this is the Seebeck effect, usually mentioned when studying the thermocouple.

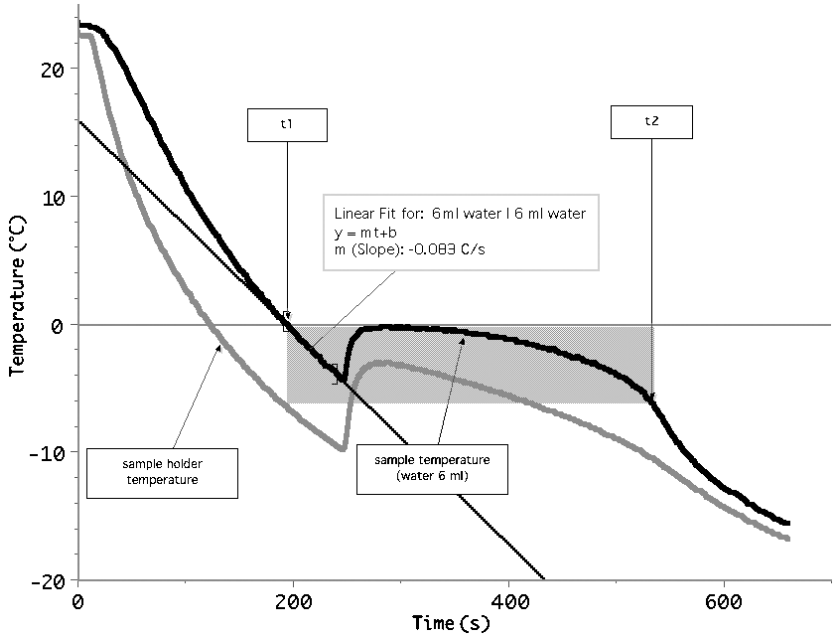

Figure 10. Cooling run, with $I = 1.8$ A with a water sample; $m = 6$ g, $t_1 = 198$ s, $t_2 = 540$ s, $S_1 = 0.083$ °C s^{-1}.

By measuring the power spent by the power supply (the product $W = IV$) during the cooling/heating run, and the same quantity while driving the propeller, the students may get an idea of the small efficiency of the complete energy transformation: less than 1% of the electrical power spent by the power supply is converted into power used by the motor [17].

For example, in the run shown in figure 2 the power source supplies about 15.4 W during 1210 s of cooling, thus dissipating about $E_1 = 18.6$ kJ of electrical energy. On the other hand, the system gained the free energy H_1 by cooling 12 g of water from the initial temperature $T_1 = 21$ °C to 0 °C, then H_2 by cooling 12 g of ice from 0 °C to $T_2 = -21$ °C. Because also the aluminium sample holder was cooled, we may optimistically evaluate an extra gain in enthalpy H_3 for cooling from T_1 to T_2 a mass equivalent to the calculated heat capacity $C_x = 45$ J °C^{-1}.

The total gain in enthalpy (using the water specific heat $c_w = 4.18$ J g^{-1} °C^{-1} and the ice specific heat $c_i = 2.04$ J g^{-1} °C^{-1}) was therefore at maximum $H = H_1 + H_2 + H_3 = 7.5$ kJ, with an energy loss of about $E_1 - H = 11.1$ kJ. We may note that more than 50% of the enthalpy is related to the latent heat.

The efficiency of the electro thermal conversion was about $H/E_1 = 40\%$.

During the heating shown in figure 2 the Peltier module was connected to the motor and we measured a starting voltage across the motor winding of about 1.9 V with a current of about 0.05 A, corresponding to a starting $W_{out} = IV = 0.1$ W. However, the product W_{out} was linearly decreasing with the temperature difference ΔT between hot and cold plates. The propeller in fact stopped rotating about at the time $t = 2600$ s, when the electrical power output due to the Seebeck effect became comparable with the friction losses.

Even assuming a constant power output equal to the initial W_{out} for the full heating curve lasting about 1600 s, the enthalpy converted into electrical energy would be about E_2 0.15 kJ, with an efficiency E_2/H of about 2%.

The overall efficiency of the two processes was therefore less than 1%.

7. Conclusions

We designed this apparatus in order to use it with our students in an introductory undergraduate course next year. Therefore we do not have yet checked it within a real course. However, the tests we made show that it offers a wide range of didactical applications. It may be used both for qualitative and quantitative investigations, substituting the traditional devices for heating/cooling. Its use is quite simple and easy, allowing us to study the *dynamics* of several phenomena in thermodynamics, exploiting a real-time data acquisition system.

We have shown some examples, beginning with the classic phase change experiment (water/ice/water), adding the possibility of easy evaluation of the thermal exchanges occurring during the phase transitions, allowed by the simultaneous use of three temperature sensors.

The device outputs experimental plots which are complex and rich of information, and quite reproducible, suitable for analysis at different levels (depending on the didactic goals of the teacher and on the age of the students).

The experiments with binary mixtures (either water/salt or water/ethanol) may also be easy performed, adding information on metastable states, which are rarely studied in textbooks. We added also one example on latent heat evaluation derived from the analysis of the cooling curves.

The proposed examples should suggest more activities aimed at improving the students ability in focusing a phenomenon and interpreting the experimental result within the frame of theoretical models.

References

[1] Güemez J, Fiolhais C and Fiolhais M 2002 Reproducing Black's experiments: freezing point depression and supercooling of water *Eur. J. Phys.* **23** 83–91
Güemez J, Fiolhais C and Fiolhais M 2002 Revising the Black's experiments on the latent heat of water *Phys. Teach.* **40** 26–31
[2] Vali G 1971 Supercooling of water and nucleation of ice *Am. J. Phys.* **39** 1125–8
[3] Menon N 1999 A simple demonstration of a metastable state *Am. J. Phys.* **67** 1109–10
[4] Kraftmakher Y 2005 Simple experiments with a thermoelectric module *Eur. J. Phys.* **26** 959–67
[5] Similar devices are produced by Melcor Corporation http://www.melcor.com (model CP 1.4-127-10L), or by Beijng Huimao Cooling Equipment Co. http://www.huimao.com (model TEC1-12704T125)
[6] Branca M and Soletta I 2005 Thermal expansion: using calculator-based laboratory technology to observe the anomalous behaviour of water *J. Chem. Educ.* **82** 613–5
[7] Andersen E S, Jespergaard P and Østersgard O 1985 *Data Book* (Pordenone: Studio Tesi Ed.) p 124
[8] Güémez J, Fiolhais C and Fiolhais M 2005 Quantitative experiments on supersaturated solutions for the undergraduate thermodynamics laboratory *Eur. J. Phys.* **26** 25–31
[9] Hoare J P 1960 Freezing point measurement *J. Chem. Educ.* **37** 146–7
[10] Han B, Hwan C J, Dantzig J A and Bischof J C 2006 A quantitative analysis on latent heat of an aqueous binary mixture *Cryobiology* **52** 146–51
[11] Atkins P 1998 *Physical Chemistry* (Oxford: Oxford University Press)
[12] Washburn E W 1928 *International Critical Tables of numerical Data, Physics, Chemistry and Technology* vol III (New York: McGraw-Hill) p 326
[13] http://homedistiller.org/calc.htm
[14] Mak S Y and Chun C K W 2000 *Phys. Educ.* **35** 181–6
[15] Gupta V K, Shanker G, Saraf B and Sharma N K 1984 Experiment to verify the second law of thermodynamics using a thermoelectric device *Am. J. Phys.* **52** 625–8
[16] Cvahte H and Strnad J 1988 A thermoelectric experiment in support of the second law *Eur. J. Phys.* **9** 11–7
[17] Gordon J M 1991 Generalized power versus efficiency characteristics of heat engines: the thermoelectric generator as an instructive illustration *Am. J. Phys.* **59** 551–5